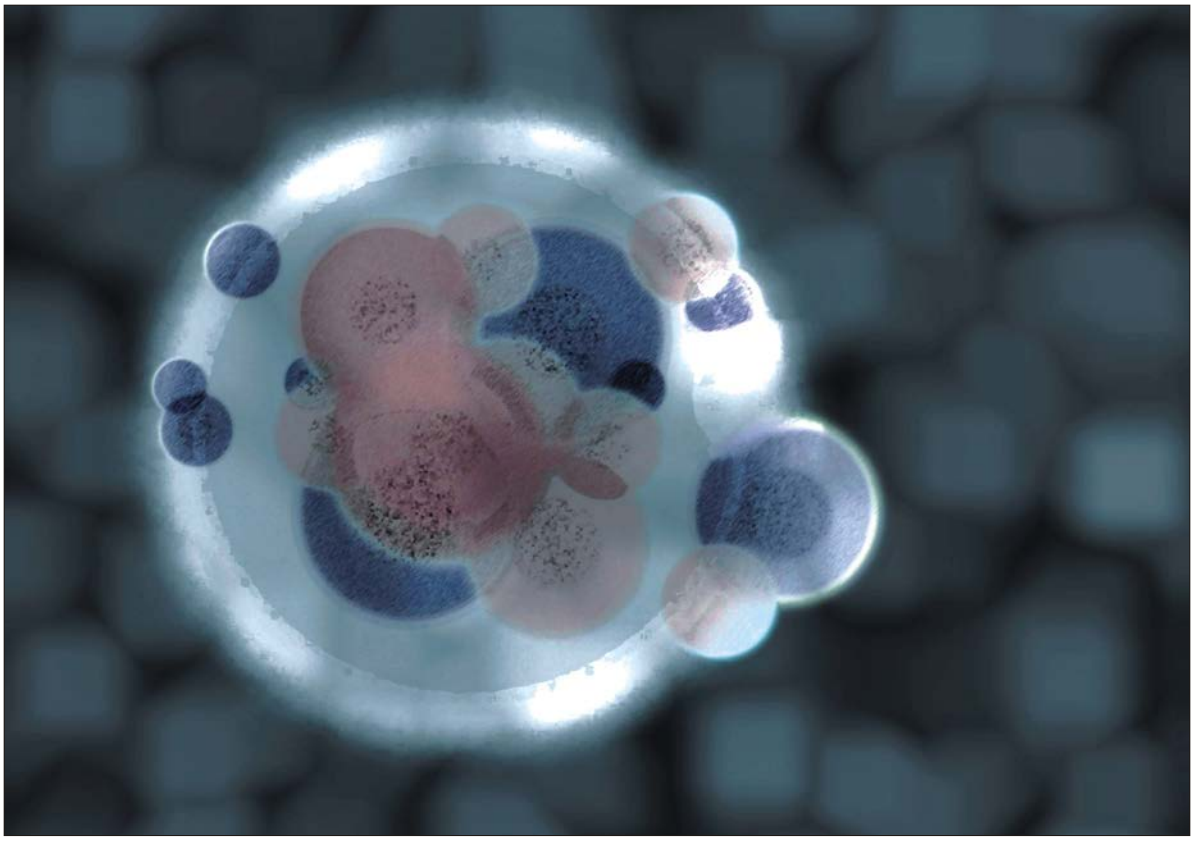

Journal of Biological Sciences

ISSN 1727-3048

science alert

ANSInet
an open access publisher
http://ansinet.com

Journal of Biological Sciences 6 (2): 231-237, 2006
ISSN 1727-3048

Quantitative Evaluation of the Skin Heat Transfer Characteristics Subjected to a Transient High-speed Helium Gas Impingement

Yi Liu
Department of Engineering Science, University of Oxford, United Kingdom

Abstract: This study is concerned with the heat transfer and aerodynamics of a needle-free epidermal powdered delivery system (biolistic system). Numerical simulations of a transient impinging jet being issued from a biolistic device have been performed to study momentum and heat transfer characteristics, with an emphasis on the gas properties immediately above a skin target. It is found that during the operation the impingement heat transfer is very unsteady. The starting process dominates features of the flow and heat transfer as it approaches the skin target. The effects of this impinging jet on the human skin are subsequently explored by a one-dimensional convection heat transfer model. Spatial-temporal characteristics of skin heat transfer are analysed and demonstrated the temperature fluctuations in the epidermal layer of skin are negligible (<1°C). These quantitative results indicate the biolistic system is patient-friendly and pain-free, apart from the unique epidermal vaccination capability.

Key words: Biolistics, heat transfer, numerical, skin, supersonic, unsteady

INTRODUCTION

Historically, drug delivery has taken the form of injection, infusion, ingestion and inhalation, with additional variations of each category (Cross and Roberts, 2004). For instance, inhalation may be via use of a dry powder inhaler, an MDI, or a nebulizer. The challenge for both the drug and drug delivery is to deliver both existing and emerging drug technologies in a manner that improves and benefits to the patients, healthcare workers and the healthcare system. Considerations identified for device development include: improved efficacy; reduced side effects; continuous dosing (sustained release); reduced pain from administration; increased ease of use; increased use compliance; improved mobility; decreased involvement of healthcare works; improved safety for healthcare workers; and reduced environment impact (elimination of CFC's).

To realize these benefits, a number of approaches are being developed. In Oxford university, we developed a novel needle-free transdermal delivery system, called biolistics, to deliver powdered vaccines into specific layers of the skin (Bellhouse *et al*., 1994; Liu *et al*., 2002a; Kendall, 2002). Figure 1 shows schematically a prototype biolistic device, configured for clinical use. Prior to operation, the high-pressure helium gas is stored in a micro-cylinder with powdered vaccines between the two thin diaphragms of a cassette. Operation commences with the opening of the helium bottle and the subsequent diaphragm rupture initiating a transonic gas flow accelerating particles to penetrate the outer layer of the skin target.

This biolistic system has been applied to many applications, including powdered drug delivery (Burkoth *et al*., 1999) and DNA vaccination (Chen *et al*., 2002). Of particular interest, we target Langerhans cells, populated with a high density in the viable epidermis, usually within 60 μm of the skin surface. Consequently, this tightly defined location makes Langerhans cells very difficult to target directly with the needle and syringe for DNA vaccination. However, the biolistics can effectively target the Langerhans cells. This unique targeting of immunologically sensitive cells shows great promise to a range of new and improved vaccinations for a range of diseases. The ballistic interaction of particles with the human, porcine and murine skin targets has been examined experimentally and analytically

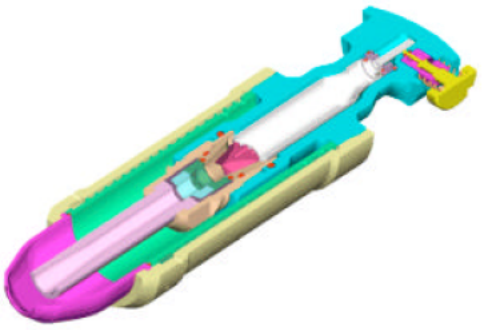

Fig. 1: A schematic of prototype biolistic device

(Kendall *et al*., 2004; Mitchell *et al*., 2003; Mulholland *et al*., 2002). However, investigations of the impinging gas-jet interaction with the skin have been limited to surface deflections from the impinging pressure. Particularly, the temperature distribution of the gas jet above the tissue target and the subsequent heat transfer are poorly understood. To explore this technology in the drug delivery applications, these issues need to be addressed thoroughly.

Meeting the requirements for better bioavailability and benefits to the patients, it is essential to provide quantitative information on the skin temperature fluctuation. In this study, we apply numerical approach to explore the temperature distribution of an impinging gas jet above the tissue surface and the skin heat transfer. Key characteristics are presented and discussed.

MATERIALS AND METHODS

Numerical approach: In order to model the impingement heat transfer process and the gas-particle interaction, flow, geometry and boundary conditions are to be established. In particular, the turbulent flow must be accurately resolved to obtain a reliable heat transfer prediction (Webb and Ma, 1995).

An efficient numerical method, based on a Modified Implicit Flux Vector Splitting (MIFVS) solver for Reynolds averaged Navier-stokes equations (RANS), has been developed and successfully applied to many different cases (Liu, 1996; Liu *et al*., 1997; 2000b; Liu and Bellhouse, 2005). Importantly, this numerical code has been the establishment of an implicit difference scheme and eigenvalue analysis of the matrix for the Navier-Stokes equations. Compared to conventional implicit methods, the MIFVS is a Jacobian spectral radius scheme and a non-approximate- factorization scheme. Since matrix operation is not needed, the amount of computing work in each time step can be significantly reduced. It has been demonstrated that the current implicit formulation is adequately efficient when applied to FVS methods, while maintaining a high level of accuracy and robustness.

The simulation of the particle acceleration requires the flow information as well as the variation of the drag coefficient with relative Reynolds and Mach numbers. The flow field can be obtained by solving the RANS equations. In this study, the drag correlation from Igra and Takayama (Igra and Takayama, 1993) was adopted due to the successful application in the previous similar biolistic system simulations (Liu *et al*., 2002a; Liu and Kendall, 2004; Liu and Costigan, 2005).

Validation: Considered the complexity and relevance to the biolistic problem, a highly under-expanded impingement jet was firstly simulated as a test case for the validation purpose (Rahimi *et al*., 2003).

Figure 2 shows the simulated wall temperature, compared with reported experimental measurements. Unlike in a low speed jet flow, the adiabatic wall temperature changes. The stagnation temperature on the unheated wall is higher than ambient temperature. As the radius increases, the adiabatic wall temperature decreases (the minimum of 14.5°C) due to the cooling effect of the high-speed jet, before it increases to ambient. The resulting Nusselt number (Nu) is plotted in Fig. 2, too. At the stagnation region, some discrepancies arise between the calculation and measurements. However, in general agreement is good, with both calculation and experiment exhibiting a monotonically decreasing Nusselt number normalized by Re^n (n = 0.52).

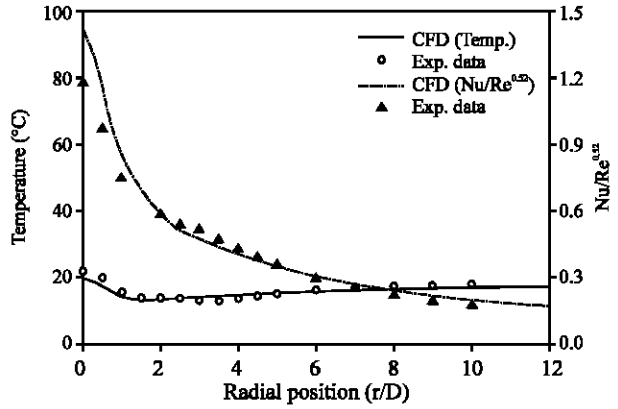

Fig. 2: Comparisons of calculated and measured temperature and corresponding normalized Nusselt number for the experimental test case (Rahimi *et al*., 2003)

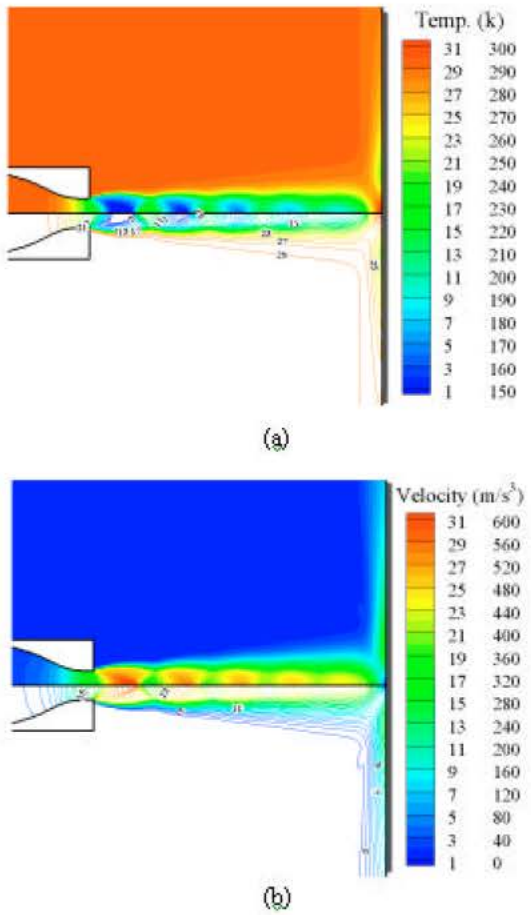

Fig. 3: Calculated contour plot of temperature (a) and velocity magnitude (b) for the experimental test case (Rahimi *et al*., 2003)

The simulated contour plots of temperature and velocity magnitude for the test case upstream of the impinging plate are shown in Fig. 3. The shock structure, subsonic zone and decay of the jet are clearly observed, with colour and line illustrating different region, which is quite similar to the schematics of Schlieren photography (Rahimi *et al*., 2003).

The good agreement in temperature and normalized Nusselt number (Fig. 2) and flow structure (Fig. 3) with the experimental data validates the implemented MIFVS code and allows us to calculate the transient temperature field with confidence.

RESULTS AND DISCUSSION

Configuration of the biolistic system: The validated numerical MIFVS code is then applied to simulate the biolistic system. The configuration of prototype device in this study is illustrated schematically in Fig. 4. This configuration was chosen because it has the most complete experimental (Kendall, 2002) and numerical (Liu *et al*., 2002a) data.

Transient gas flow field of the biolistic system: Figure 5 presents a sequence of temperature contours after diaphragm rupture. Key flow features, such as the propagation of the primary shock, contact surface, hot gas (driven air gas in Region 2), cold gas (driver helium-air in Region 3) and the secondary shock, are shown from a time of 98 μs after diaphragm rupture. The high temperature zone just above the target establishes when the primary shock reaches and is interacted with the skin target from a time of 106 μs. The high temperature zone becomes thinner at a time of 148 μs, indicating a standing normal-shock-like wave is formed following the unsteady expansion. At a time of 194 μs, shown the termination of

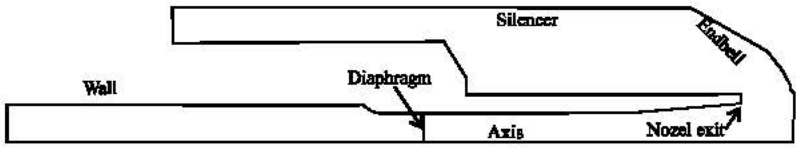

Fig. 4: Configuration of prototype biolistic device

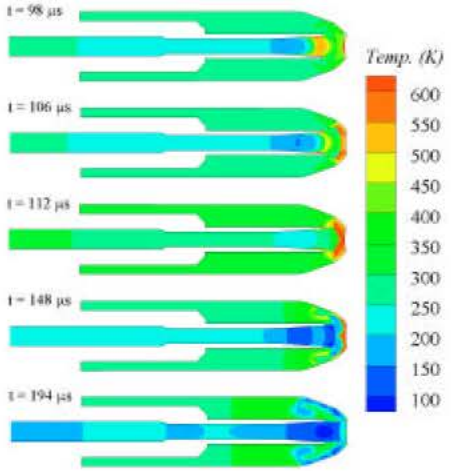

Fig. 5: Time sequence of simulated temperature contours

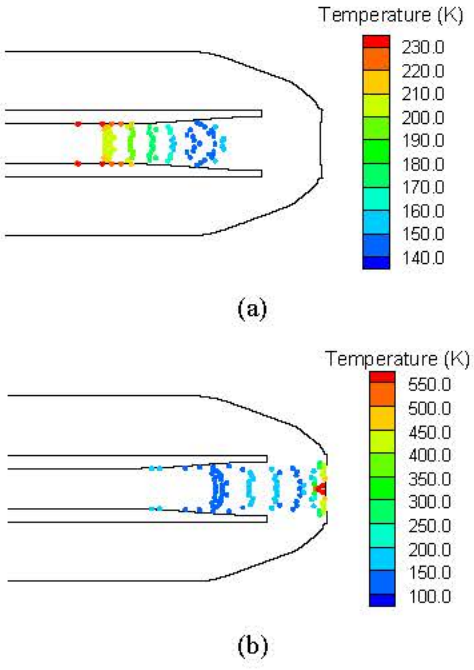

Fig. 6: Calculated particle temperature map at a time of 112 μs (a) and 148 μs (b)

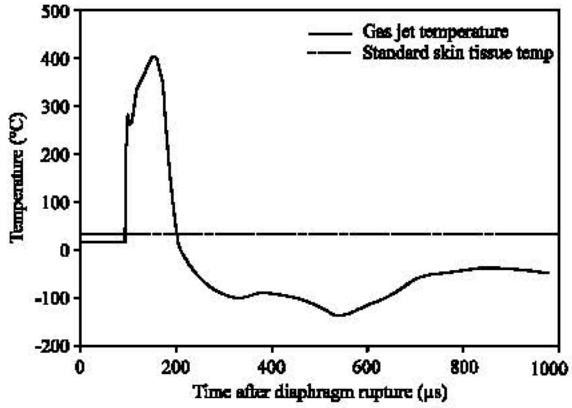

Fig. 7: Gas temperature histories averaged at the impingement surface

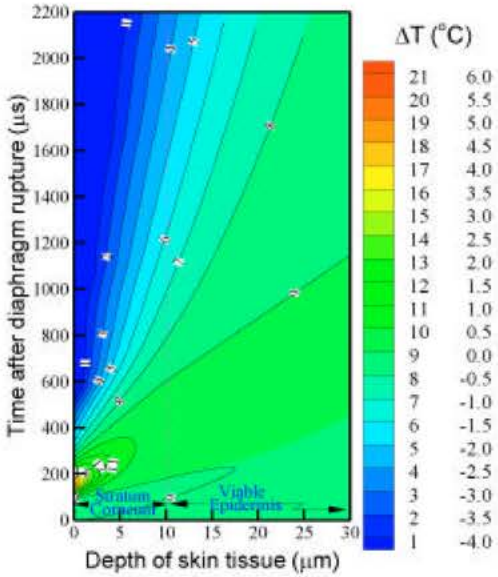

Fig. 8: Calculated space-time (X-T) temperature fluctuation contours

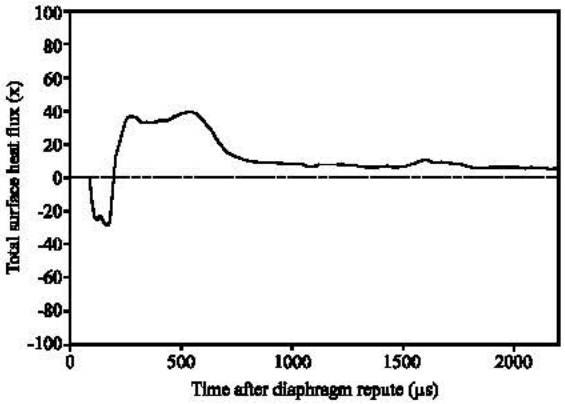

Fig. 9: Calculated total surface heat flux history

the starting process. The cold gas arrives at the skin. A quasi-steady supersonic flow regime is established, which is preferable for the vaccine delivery.

Particle characteristics of the biolistic system: The gas-particle dynamics and heat transfer were predicted with simulation of gas-particle-target interactions. The typical temperature variations for particles at 112 and 148 μS after diaphragm rupture are shown in Fig. 6, respectively. Not surprisingly, the particles undergo large temperature variations during the delivery process. Those simulations provide a valuable guideline for the vaccine reformulation and coating process.

Impingement temperature characteristics: Simulated gas temperature evolutions above the skin are plotted in Fig. 7. The shown temperature is averaged over the skin surface area covered. It is found that during the operation the impingement temperature is very unsteady. The starting process dominates features of the flow and heat transfer as it approaches the skin target.

Skin heat transfer: Simulated results in Fig. 5 and 7 clearly illustrate a large change in key gas parameters above the skin surface. Now we turn our attention to the skin temperature fluctuation, resulting from heat transfer between the skin and the transient high-speed gas jet.

To address this issue, a simplified heat transfer model, which does not consider the complexity of human body temperature regulation, is developed. The human skin surface is exposed to a convection-surface environment of a transient gas impingement jet. The initial skin temperature is set at the normal level of 34°C, reported in the literature (Skin Website). A two-layer model (Mulholland *et al*., 2002) for the skin was applied with the stratum corneum outer layer, assigned a density of 1500 kg m^{-3} and a thickness of 10.6 μm, respectively. Below, the viable epidermis and dermis density is set to 1150 kg m^{-3} with the maximum thickness of 100 μm. Other skin parameters applied to the numerical modelling are the specific heat capacity of 4180 J/kg K and thermal conductivity of 0.37 W/m K (Skin Website). An averaged gas temperature variation (plotted in Fig. 7) and a constant heat transfer coefficient of 2875 W/m^2 K were obtained from the transient gas flow calculation.

Figure 8 shows the contour plots of temperature fluctuations in the skin, following the high-speed gas jet impinging. The largest temperature fluctuations appear on the skin surface with a maximum of 5.5°C at the time of about 170 μs (corresponding to the peak impinging gas temperature, shown in Fig. 7), before cooling to a minimum of -4.0°C at 2.0 ms. This temperature decay rapidly approach the normal skin temperature before it reaches the dermis. Deeper into the skin, the temperature fluctuations are much lower.

It is clearly exhibited the maximum fluctuation is less than 1°C, in the depth of 10.6 μm below skin surface (i.e., the thickness of the stratum corneum) and within a time of 1.0 ms for the vaccine delivery. The temperature fluctuation in the viable epidermis is negligible. These results are consistent with clinical trials of biolistic delivery (Swain *et al*., 2000), in which patients report no sensation of pain.

Figure 9 shows a total surface heat flux history. As a result of the impinging jet, the total net heat of 1.53×10^{-2} J is lost from the skin into environment. As an illustration, an adult male (even when inactive), the heat loss is at a rate of about 90 watts as a result of basal metabolism. Therefore, these calculations suggest that heat transfer from the impinging jet has a negligible effect on patient discomfort and changes in the ballistic input process.

CONCLUSIONS

Transient aerodynamics and heat transfer from biolistic system have been investigated numerically. The simulation has firstly been validated and demonstrated to be numerically accurate, efficient and robust. Results obtained for the wall surface temperature, shock structures and the heat transfer show good agreements with the experimental data and other published calculation results.

The transient flow and temperature simulations within a biolistic device show that the starting process dominates the jet impingement heat transfer. Spatial-temporal behaviour of the heat transfer has been analysed in terms of the instantaneous temperature variations of the supersonic jet and entrained particles.

A one-dimensional convection heat transfer calculation has been performed and found the temperature fluctuation in the viable epidermis is negligible. Therefore, the heat transfer between the biolistic jet and skin is insignificant. The quantitative result is consistent with the pain-free clinical trial observations.

Subsequent computations need to be further explored to assess the effects of important parameters such as jet-to-target distance, endbell geometry and Reynolds number, as well as to examine the influence of jet confinement and nozzle-exit profiles.

ACKNOWLEDGMENT

Professor Brian J. Bellhouse and Dr. Mark A.F. Kendall are acknowledged for their insights and suggestions.

REFERENCES

Bellhouse, B.J., D.F. Sarphie and J.C. Greenford, 1994. Needless syringe using supersonic gas flow for particle delivery. Intl. Patent WO94/24263.

Burkoth, T.L., B.J. Bellhouse, G. Hewson, D.J. Longridge, A.G. Muddle and D.F. Sarphie, 1999. Transdermal and transmucosal powdered drug delivery. Crit. Rev. Ther. Drug Carrier Sys., 16: 331-384.

Chen, D., Y. Maa and J.R. Haynes, 2002. Needle-free epidermal powder. Expert. Rev. Vaccines, 1: 89-100.

Cross, S.E. and M.S. Roberts, 2004. Physical enhancement of transdermal drug application: Is delivery technology keeping up with pharmaceutical development? Current Drug Delivery, 1: 81-92.

Igra, O. and K. Takayama, 1993. Shock tube study of the drag coefficient of a sphere in a non-stationary flow. Proc R. Soc. Lond. A, 442: 231-247.

Kendall, M.A.F., 2002. The delivery of particulate vaccines and drugs to human skin with a practical, hand-held shock tube-based system. Shock Waves J., 12: 22-30.

Kendall, M.A.F., S. Rishworth, F. Carter and T.J. Mitchell, 2004. Effects of relative humidity and ambient temperature on the ballistic delivery of micro-particles to excised porcine skin. J. Investigative Dermatol., 122: 739-746.

Liu, Y., 1996. Numerical method of three-dimensional viscous flow in turbomachinery multistage environment. Ph.D Thesis, Xi'an Jiaotong University, China.

Liu, Y., Q. Cao and Y.M. Xiang, 1997. Numerical simulation of viscous flows in transonic diffuser. J. Hydrodynamics, Ser. A, 12: 33-37.

Liu, Y., M.A.F. Kendall, N.K. Truong and B.J. Bellhouse, 2002a. Numerical and experimental analysis of a high speed needle-free powdered vaccines delivery device, AIAA-2002-2807. In Proceeding 20th AIAA Applied Aerodynamics Conference, St. Louis, MO, USA.

Liu, Y., M.A.F. Kendall and B.J. Bellhouse, 2002b. An efficient implicit finite-difference scheme for transonic flow. AIAA 2002-2955, 32nd AIAA Fluid Dynamics Conference and Exhibit, St. Louis, Missouri, USA.

Liu, Y. and M.A.F. Kendall, 2004. Numerical study of a transient gas and particle flow in a high-speed needle-free ballistic particulate vaccine delivery system. J. Mech. Med. Biol., 4: 559-578.

Liu, Y. and B.J. Bellhouse, 2005. Prediction of jet flows in the supersonic nozzle and diffuser. Intl. J. Num. Methods in Fluids, 47: 1147-1155.

Liu, Y. and G. Costigan, 2005. Aerodynamic performance of an earlier Venturi powdered vaccines/drug delivery system. AIAA-2005-5005, Proc. 35th AIAA Fluid Dynamics Conference and Exhibit, Toronto, Canada.

Mitchell, T.J., M.A.F. Kendall and B.J. Bellhouse, 2003. A ballistic study of micro-particle penetration to the oral mucosa. Intl. J. Impact Eng., 28: 581-599.

Mulholland, W.M., M.A.F. Kendall, B.J. Bellhouse and N. White, 2002. Analysis of microparticle penetration into human and porcine skin: Non-invasive imaging with multiphoton excitation microscopy, SPIE Microscopy International Conference, San Jose, California, USA.

Rahimi, M., I. Owen and J. Mistry, 2003. Impingement heat transfer in an under-expanded axisymmetric air jet. Intl. J. Heat and Mass Transfer, 46: 263-272.

Skin website, 2001. http://hypertextbook.com/facts/2001/AbantyFarzana.shtml.

Swain, W.E. and D. Heydenburg Fuller, 2000. Tolerability and immune responses in humans to a PowderJect DNA vaccine for hepatitis B. Dev. Biol., 104: 115-119.

Webb, B. and C.F. Ma, 1995. Single-phase liquid jet impingement heat transfer. Advances in Heat Transfer, 26: 105-217.